

Relationship of GDF15 with hepatic mitochondrial respiration is depending on the presence of fibrosis in obese individuals

Anna Giannakogeorgou, Sabine Kahl, Cesare Granata, Geronimo Heilmann, Lucia Mastrototaro, Bedair Dewidar, Pavel Bobrov, Irene Esposito, Aslihan Yavas, Sandra Trenkamp, Frank A. Granderath, Matthias Schlensak, Christos S. Mantzoros, Michael Roden, Patrick Schrauwen

Article - Version of Record

Suggested Citation:

Giannakogeorgou, A., Kahl, S., Granata, C., Heilmann, G., Mastrototaro, L., Dewidar, B., Bobrov, P., Esposito, I., Yavas, A., Trenkamp, S., Granderath, F. A., Schlensak, M., Mantzoros, C. S., Roden, M., & Schrauwen, P. (2025). Relationship of GDF15 with hepatic mitochondrial respiration is depending on the presence of fibrosis in obese individuals. Metabolism, 173, Article 156391. https://doi.org/10.1016/j.metabol.2025.156391

Wissen, wo das Wissen ist.



This version is available at:

URN: https://nbn-resolving.org/urn:nbn:de:hbz:061-20251023-124813-5

Terms of Use:

This work is licensed under the Creative Commons Attribution 4.0 International License.

For more information see: https://creativecommons.org/licenses/by/4.0



Contents lists available at ScienceDirect

Metabolism

journal homepage: www.journals.elsevier.com/metabolism





Relationship of GDF15 with hepatic mitochondrial respiration is depending on the presence of fibrosis in obese individuals

Anna Giannakogeorgou ^{a,b,1}, Sabine Kahl ^{a,b,c}, Cesare Granata ^{a,b}, Geronimo Heilmann ^{a,b}, Lucia Mastrototaro ^{a,b}, Bedair Dewidar ^{a,b}, Pavel Bobrov ^{b,d}, Irene Esposito ^e, Aslihan Yavas ^e, Sandra Trenkamp ^{a,b}, Frank A. Granderath ^f, Matthias Schlensak ^f, Christos S. Mantzoros ^g, Michael Roden ^{a,b,c,2,*}, Patrick Schrauwen ^{a,b,2,**}

- a Institute of Clinical Diabetology, German Diabetes Center, Leibniz Institute for Diabetes Research at Heinrich Heine University, Düsseldorf, Germany
- ^b German Center for Diabetes Research (DZD e.V.), Partner Düsseldorf, München-Neuherberg, Germany
- c Department of Endocrinology and Diabetology, Faculty of Medicine and University Hospital, Heinrich Heine University, Düsseldorf, Germany
- d Institute for Biometrics and Epidemiology, German Diabetes Center, Leibniz Center for Diabetes Research at Heinrich Heine University, Düsseldorf, Germany
- ^e Institute of Pathology, Medical Faculty, Heinrich-Heine University Düsseldorf, Düsseldorf, Germany
- f Adipositas- und Refluxzentrum, Krankenhaus Neuwerk, Mönchengladbach, Germany
- ⁸ Department of Medicine, Beth Israel Deaconess Medical Center, Harvard Medical School, Boston, MA 02215, United States of America; Boston VA Healthcare System, Harvard Medical School, Boston, MA, United States of America

ARTICLE INFO

Keywords:
Growth differentiation factor 15
Obesity
Insulin resistance
Mitochondria
Liver
Fibrosis

ABSTRACT

Background and purpose: Preclinical studies reported elevated growth differentiation factor 15 (GDF15) when mitochondrial function is reduced. In humans, metabolic dysfunction-associated steatotic liver disease (MASLD) and steatohepatitis (MASH) exhibit different hepatic mitochondrial adaptation. We hypothesized that circulating GDF15 differently correlates with hepatic mitochondrial respiration in obesity and/or MASLD/MASH. *Methods*: Humans without (n = 20) and with biopsy-confirmed MASLD (n = 20) or MASH (n = 20) underwent

Methods: Humans without (n = 20) and with biopsy-confirmed MASLD (n = 20) or MASH (n = 20) underwent hyperinsulinemic-euglycemic clamps to assess whole-body (M-value) and adipose-tissue (insulin-induced NEFA suppression) insulin sensitivity. Fasting serum GDF15 and glucagon were quantified by ELISA. Mitochondrial respiration was measured in liver obtained during bariatric surgery by high-resolution respirometry. Associations were assessed with Spearman's nonparametric correlation.

Results: Serum GDF15 correlated negatively with M-value (r=-0.35, p=0.017) and NEFA suppression (r=-0.29, p=0.046), but not with hepatic mitochondrial respiration across the whole cohort. However, correlations were found upon stratification into groups based on the presence (n=37, age: $41\pm 2y$, BMI: 49 ± 1 kg/m²) or absence of hepatic fibrosis ($n=23, 44\pm 2$ years, BMI: 49 ± 1 kg/m²). In persons without fibrosis, GDF15 correlated positively with fatty acid oxidation-linked (F_P ; r=0.35, p=0.035) and maximal coupled (FNS_P; r=0.42, p=0.010) mitochondrial respiration. Conversely, GDF15 correlated negatively with hepatic FN_P in persons with fibrosis (r=-0.48, p=0.022).

Abbreviations: Adipo-IR, adipose tissue insulin resistance index; ATF4, activating transcription factor 4; BMI, body mass index; Cpt2, carnitine palmitoyl-transferase 2; F, fatty acid oxidation; F_L, leak respiration (L) with electron input through the F pathway; FN_P, P with electron input through the F and N pathways combined; FNS_E, electron transport chain capacity (E) with electron input through the F, N, and S pathways combined; FNS_P, P with electron input through the F, N, and S pathways combined; FP, OXPHOS capacity (P) with electron input through the F pathway; GDF15, growth differentiation factor 15; HOMA-IR, Homeostatic Model Assessment of Insulin Resistance; HRR, high-resolution respirometry; MASH, metabolic dysfunction-associated steatohepatitis; MASLD, metabolic dysfunction-associated steatotic liver disease; N, NADH, nicotinamide adenine dinucleotide; NEFA, non-esterified fatty acids; N_L, L with electron input through the N pathway; N_P, P with electron input through the N pathway; NS_E, E with electron input through the N and S pathways combined; OXPHOS, oxidative phosphorylation; P, OXPHOS capacity; S, succinate; SAT, subcutaneous adipose tissue; VAT, visceral adipose tissue.

^{*} Correspondence to: M. Roden, Department of Endocrinology and Diabetology, Faculty of Medicine and University Hospital, Heinrich Heine University Düsseldorf, c/o Auf m Hennekamp 65, 40225, Düsseldorf, Germany.

^{**} Correspondence to: P. Schrauwen, Institute of Clinical Diabetology, German Diabetes Center, Auf'm Hennekamp 65, 40225, Düsseldorf, Germany. *E-mail addresses*: michael.roden@ddz.de (M. Roden), patrick.schrauwen@ddz.de (P. Schrauwen).

¹ Present address: Department of Internal and Vascular Medicine, Amsterdam University Medical Centers, University of Amsterdam, Amsterdam, the Netherlands.

² These authors share last authorship.

Conclusions: In humans with obesity, serum GDF15 correlates positively with hepatic mitochondrial respiration in persons without, but negatively in persons with hepatic fibrosis. Future studies are needed to investigate whether and how GDF15 affects hepatic mitochondrial respiration in a fibrosis-dependent manner and/or, conversely, how fibrosis might modulate hepatic GDF15 secretion through altered mitochondrial function.

1. Introduction

Growth differentiation factor 15 (GDF15) is secreted by various tissues and decreases appetite and food intake with mild weight loss by acting through the glial cell-derived neurotrophic factor family receptor alpha-like (GFRAL) [1-3]. In humans, circulating GDF15 levels are elevated in obesity and further increased in obesity-associated type 2 diabetes [4]. Under these conditions, the adipose tissue becomes the main source of circulating GDF15 [5]. The seemingly paradoxical GDF15 secretion could serve as a compensatory mechanism to overcome obesity-related metabolic disturbances such as insulin resistance. Indeed, there is some evidence for a positive relationship between circulating GDF15 levels and surrogates of insulin sensitivity [6,7]. Next to obesity and type 2 diabetes, circulating GDF15 can be even further elevated in humans with metabolic dysfunction-associated steatotic liver diseases (MASLD) [8-12], specifically in advanced MASLD such as metabolic dysfunction-associated steatohepatitis (MASH) and in the presence of fibrosis [5,9-11]. Recent evidence suggests that the liver contributes to circulating GDF15 in humans with MASH [5]. Interestingly, the liver also appears to be the predominant source of serum GDF15 in obese high-fat diet-fed mice [13].

In obesity, insulin resistance and/or MASLD, various alterations of mitochondrial oxidative capacity can occur, e.g. in liver [14], skeletal muscle [15] and adipose tissue. In rodents, GDF15 can stimulate energy expenditure and mitochondrial respiration [16-18]. GDF15 is also markedly increased in transgenic mouse models with altered mitochondrial oxidative capacity in liver [19,20], adipose tissue [21] or skeletal muscle [16], as well as in naturally aging mice exhibiting reduced skeletal muscle mitochondrial respiration and impaired insulin sensitivity [22]. This suggests a negative feedback loop between mitochondrial function and GDF15 secretion helping to restore oxidative capacity and insulin sensitivity. Furthermore, recombinant GDF15 treatment or transgenic GDF15 overexpression in rodents has been demonstrated to ameliorate hepatic steatosis and fibrosis [17,23-25]. Thus, GDF15 is currently considered a putative therapeutic agent for the treatment of obesity-related metabolic complications, such as MASLD [26-30].

At present, there is no data on a relationship between circulating GDF15 concentrations and tissue-specific insulin sensitivity as determined by a gold-standard method such as the hyperinsulinemiceuglycemic clamp test. Further it is unknown whether GDF15 associates with tissue-specific mitochondrial function in humans, which is mainly due to restricted access to some of these tissues in humans. Thus, we tested the hypothesis that circulating GDF15 levels (i) are related to mitochondrial oxidative capacity in different tissues and (ii) correlate with tissue-specific insulin sensitivity in humans with obesity and/or MASLD/MASH. Since recent human studies have suggested that glucagon increases circulating GDF15 levels, particularly in MASLD [31], we included glucagon in our analysis. To test these hypotheses, we made use of the BARIA-DDZ cohort, which provides liver histology, multiple tissue biopsies to measure mitochondrial respiration ex vivo and hyperinsulinemic-euglycemic clamp tests to assess insulin sensitivity in vivo.

2. Methods

2.1. Study participants

This cross-sectional study included Caucasian individuals from the

BARIA-DDZ Study (ClinTrials.gov: NCT01477957), which includes participants with obesity undergoing bariatric surgery. The participants of this analysis were selected based on availability of hepatic mitochondrial respiration data and suitable serum samples. All participants underwent liver biopsies during bariatric surgery, which allowed identification of three groups based on liver histology: obesity without liver steatosis, defined by lipid content <5 % and/or steatosis grade 0 (OBECON, n=20), obesity with MASLD (OBE-MASLD, n=20) and obesity with MASH (OBE-MASH, n=20) (Table 1). MASLD was defined as liver steatosis (lipid content ≥ 5 % and/or steatosis grade ≥ 1) without hepatocyte ballooning. MASH was defined by liver steatosis and combined lobular inflammation plus hepatocyte ballooning, as previously described [32]. Participants with liver disease other than MASLD were excluded.

2.2. Ethical considerations

Prior to inclusion, informed consent to the study protocol upon information about the procedures and potential risks was obtained from all participants. The study was approved by the ethics boards of Heinrich-Heine-University Düsseldorf and of the Medical Association North Rhine (no. 2022-2021_1-andere Forschung erstvotierend/no. 2017222) and conducted in accordance with the ethical standards as set down in the 1964 Declaration of Helsinki and its latest amendment (2013).

2.3. Study design

Before bariatric surgery, participants underwent a hyperinsulinemiceuglycemic clamp to measure insulin sensitivity and blood was collected for lab analyses. Skeletal muscle and subcutaneous adipose tissue biopsies were collected immediately before starting the clamp, whereas visceral adipose tissue and liver biopsies were obtained during surgery.

2.4. Hyperinsulinemic-euglycemic clamp test

Whole-body and hepatic insulin sensitivity was assessed via a three-hour hyperinsulinemic-euglycemic clamp. During the clamp (start $t=180\,$ min), blood glucose was maintained at 90 mg/dL through counterbalancing the primed-continuous insulin (Insuman Rapid, Sanofi, Frankfurt am Main, Germany) infusion (80 mU/m²/min) for 8 min followed by 40 mU/m²/min until the end of the procedure with a variable 20 % (w/v) glucose infusion (B. Braun, Melsungen, Germany) [33]. The procedure involved blood sampling in regular intervals, i.e. at t=0, 180, 240, 300, 340, 350 and 360 min for quantification of NEFA, glucose and

Table 1Liver histology.

	OBE-CON	OBE-MASLD	OBE-MASH
Steatosis grade (0/1/2/3)	20/0/0/0	0/14/3/3	0/8/9/3
Lobular inflammation $(0/1/2/3)$	8/8/4/0	4/8/7/1	0/11/8/1
Hepatocyte Ballooning (0/1/2)	16/3/1	20/0/0	0/12/8
Fibrosis Stage (0/1/2/3/4)	15/3/1/1/0	14/4/2/0/0	8/7/3/2/0
Lipid content (%)	1 [0-4]	17 [5-45]	43 [25-60]
NAFLD Activity Score (0/1/2/3/	5/9/6/0/0/	0/4/5/6/3/2/	0/0/2/6/
4/5/6)	0/0	0/0	9/3

For each histological feature, the number of study participants per score and group is presented. Lipid content is reported as median [Interquartile range (IQR)]. The overall comparison across the three groups yielded p < 0.001.

insulin, as previously described [32]. Whole-body insulin resistance (M-value) was calculated from steady-state glucose infusion rate with glucose space correction, as previously described [34]. HOMA-IR, calculated as Insulin_{fasting} [μ U/mL] * Glucose_{fasting} [mmol/L]) divided by 22.5, was used as a surrogate measure of whole-body insulin sensitivity [31] Adipose tissue insulin resistance was evaluated indirectly through calculation of the Adipo-IR index, which was calculated as NEFA_{fasting} * Insulin_{fasting} [35]. Furthermore, insulin-induced percent suppression of NEFA during the clamp was calculated as [NEFA_{fasting} – NEFA_{clamp360}·] * 100/NEFA_{fasting} [35].

2.5. Tissue biopsies

Subcutaneous adipose tissue (SAT) and skeletal muscle biopsies were obtained in the fasted state before the start of the clamp. SAT biopsies were obtained at the level of the umbilicus by needle suction under local anesthesia (5–10 mL of 1 % lidocaine) [36]. Skeletal muscle biopsies were obtained after administration of local anesthesia from the m. vastus lateralis by experienced physicians using a modified Bergström needle with suction, as previously described [33]. The biopsies were immediately blotted free of extramyocellular tissue or blood. Samples were placed in ice-cold BIOPS solution and immediately used for high-resolution respirometry (HRR) measurements. The remaining samples were weighed, snap-frozen in liquid nitrogen, and subsequently stored at $-80\,^{\circ}\text{C}$ for further analyses.

Liver biopsies were obtained intraoperatively during bariatric surgery, at 30 min after anesthesia induction, following a standardized protocol [37]. Samples were collected from the lower part of the right liver lobe. For the purposes of this study, approximately 50 mg was placed in ice-cold relaxing medium (BIOPS buffer solution) for HRR analysis, the remaining tissue was used for histological evaluation or snap-frozen in liquid nitrogen and subsequently stored at $-80\,^{\circ}\mathrm{C}$. Liver histology and MASLD staging were performed in accordance with the NASH Clinical Research Network Scoring system [38] (Table 1). MASH was diagnosed when hepatic steatosis of at least grade 1 was present in conjunction with ballooning and lobular inflammation [32].

Visceral adipose tissue (VAT) biopsies were also collected intraoperatively from the omentum majus and transferred into BIOPS solution for HRR analysis.

2.6. Liver histology

Liver biopsies were histologically evaluated according to the most recent EASL-EASD-EASO Guidelines [39], based on the presence and severity of steatosis, lobular inflammation, hepatocellular ballooning, and fibrosis, as previously described [32]. In our cohort consisting of individuals with grade III obesity, MASLD was defined by the presence of hepatic steatosis, as obesity itself constitutes a cardiometabolic risk factor [39]. MASH was defined by the concurrent presence of hepatocellular ballooning and lobular inflammation.

Steatosis grade was defined as follows: 0 (<5 %), 1 (5–33 %), 2 (33–66 %), and 3 (>66 %). Lobular inflammation was defined as: 0 (no inflammatory foci), 1 (<2 foci per $200\times$ field), 2 (2–4 foci per $200\times$ field), and 3 (>4 foci per $200\times$ field). Ballooning of hepatocytes was defined as: 0 (none), 1 (few ballooned cells) and 2 (many ballooned cells/prominent ballooning). Fibrosis staging was defined as: 0 (none), 1 (perisinusoidal/periportal) with subcategories F1A (mild, zone 3, perisinusoidal), F1B (moderate, zone 3, perisinusoidal) and F1C (portal/periportal), F2 (perisinusoidal and portal/periportal), F3 (bridging fibrosis) and F4 (cirrhosis).

Additionally, the NAFLD Activity Score (NAS), as established by the NASH Clinical Research Network [40], was calculated, as detailed in prior work [32,37].

2.7. Laboratory analyses

NEFA was quantified in blood samples collected in orlistatcontaining vials (Wako Chem USA Inc. Osaka, Japan) and measured on a Cobas C311 analyzer (Roche Diagnostics, Basel, Switzerland) as described previously [35,41]. Glucose and insulin were assessed as previously described [42].

Total GDF15 was measured in serum samples obtained after overnight fasting (t=0) using enzyme-linked immunosorbent assays (ELISAs) from Ansh Laboratories (Webster, TX, USA) [10]. Samples were measured in duplicates with coefficients of variations (CV) \leq 12 %. Concentration was calculated using a standard curve with $R^2 > 0.99$. Individual assay performance was judged using quality control samples at low and high range of the assay range provided by the manufacturer. Concentration of the quality control samples were within the target range given by the assay manufacturer. Inter-assay variability (CV), as assessed using a standard serum for each assay, was 7.6 %.

Fasting glucagon (t=0) was quantified using the Mercodia (Uppsala, Sweden) glucagon assay (10-1271-01, Lot: 35467) according to the manufacturer's protocol. Each sample was measured in duplicate and the concentrations were calculated as the mean of the duplicates. Intraassay precision was validated by quality control samples provided by the manufacturer at three concentrations (4.47, 14.4, 44.1 pmol/L) within the calibration range. Inter-assay variability assessed by coefficient of variation was 6.6 %.

2.8. Mitochondrial respiration

Fresh skeletal muscle was carefully blotted before being permeabilized by gentle agitation for 30 min at 4 $^{\circ}$ C in BIOPS containing 50 µg/mL of saponin, and three 5-min washes in MiR05 [43]. VAT and SAT samples were blotted dry and membranes were permeabilized by direct titration of digitonin (5 µg/mL) in the chamber [41]. For muscle and liver \sim 2–3 mg of tissue were used [32], and for VAT and SAT samples \sim 20 mg [41].

For all tissues, mitochondrial respiration (O2 flux rates) was measured in duplicate in MiR05 at 37 °C using the high-resolution Oxygraph-2k (Oroboros, Innsbruck, Austria). Two substrateuncoupler-inhibitor titration (SUIT) protocols [37,41,43,44] were used; the first was performed in skeletal muscle VAT, SAT, and liver and was as follows: 1 mmol/L octanoylcarnitine and 2 mmol/L malate (F_L: leak respiration [L] with electron input through the fatty acid oxidation [F] pathway); 2.5 mmol/L ADP (Fp: OXPHOS capacity [P] with electron input through the F pathway); 10 mmol/L glutamate (FN_P: P with electron input through the F and NADH (N) pathways combined); 10 mmol/L succinate (FNSP: P with electron input through the F, N, and succinate (S) pathways combined); $6 \mu mol/L$ cytochrome c to assess the outer mitochondrial membrane integrity; only in VAT and SAT: 10 nmol/L oligomycin (FNS_L: L with electron input through the F, N, and S pathways combined); 0.75-1.5 µmol/L carbonyl cyanide 4-(trifluoromethoxy) phenylhydrazone (FCCP) via stepwise titration (FNS_E, maximal electron transport chain capacity [E, noncoupled respiration] with electron input through the F, N, and S pathways combined).

The second SUIT protocol was performed in skeletal muscle and liver and was as follows: 2 mmol/L malate and 10 mmol/L glutamate (N_L: L with electron input through the N pathway); 2.5 mmol/L ADP (N_P: P with electron input through the N pathway); 10 mmol/L succinate (NS_P: P with electron input through the N and S pathways combined); 6 μ mol/L cytochrome c to assess the outer mitochondrial membrane integrity; FCCP (0.75–1.5 μ mol/L for liver and skeletal muscle; 1.5–5 μ mol/L for VAT and SAT) via stepwise titration (NS_E, E with electron input through the N and S pathways combined).

For all protocols, cytochrome c responses >15 % excluded [43], and all O₂ flux rates were expressed as pmol O₂ s⁻¹ mg⁻¹ wet weight.

Citrate synthase activity (CSA) was measured spectrophotometrically using a CSA Kit (Sigma-Aldrich, St. Louis, MO, USA), as previously

outlined [41].

2.9. Statistical analyses

Normality was assessed using the Shapiro-Wilk test. Data are presented as means \pm standard error of the mean (SEM). Between-group comparisons were performed with one-way ANOVA or Kruskal-Wallis test or with unpaired t-tests or Mann-Whitney-U tests for normally distributed and not normally distributed data, respectively. For nominal variables, such as sex or presence of type 2 diabetes, Fisher's exact test was applied to calculate differences across groups. Post-hoc tests were conducted using Tukey's HSD test following significant ANOVA results, Dunn's test following significant Kruskal-Wallis results and the Bonferroni correction for comparisons between the fibrosis and no-fibrosis groups.

Based on the skewed distribution of serum GDF15, nonparametric Spearman correlation test was performed to investigate the relationship between GDF15 and mitochondrial respiration rates. Further exploratory correlations in the entire study cohort were investigated between GDF15 and anthropometric variables, whole-body and adipose tissue insulin resistance.

Given the further increase in GDF15 levels in the presence of fibrosis [9–11], in conjunction with preclinical evidence of its anti-fibrotic effects [23–25], we stratified the cohort into two groups, namely those without fibrosis (F0) and those with fibrosis (F \geq 1). Differences in hepatic mitochondrial respiration rates between the groups were assessed by Student's t-test for independent variables for normally distributed variables and Mann-Whitney-Used test for skewed variables, and correlation analysis was performed using non-parametric Spearman correlations, due to the skewed distribution of GDF15 in both groups.

Statistical significance was set at p<0.05 for all tests. All analyses were performed with IBM SPSS Statistics Version 29.0 and GraphPad Prism Version 10.3.1 for MacOS (464). Data are presented as means \pm SEM in tables and figures, unless stated otherwise.

3. Results

3.1. GDF15 concentrations are comparable in obese individuals without MASLD, with MASLD or with MASH

Participants were divided into three groups based on their liver histology. By definition, the OBE-MASLD group showed no hepatocyte ballooning; however, some individuals showed signs of early lobular inflammation and fibrosis. MASH was defined by liver steatosis and combined lobular inflammation plus hepatocyte ballooning, as previously described [32]. Likewise, the OBE-MASH group showed both lobular inflammation and hepatocyte ballooning and only moderate fibrosis, indicating a relatively mild liver disease (Table 1).

Age, sex and BMI were comparable across the groups of obese individuals without liver steatosis (OBE-CON), with MASLD (OBE-MASLD) or with MASH (OBE-MASH) (Table 2). Liver transaminases differed across groups (Table 2). Clamp-derived whole-body and adipose tissue insulin sensitivity (M-value and %NEFA suppression), as well as fasting insulin sensitivity indices (HOMA-IR and Adipo-IR) were similar between groups (p > 0.05, Table 2). No differences in GDF15 levels were found between groups (p > 0.05, Table 2).

3.2. GDF15 correlates with whole-body and adipose tissue-specific insulin resistance

Circulating GDF15 correlated positively with age, but not with BMI (Fig. 1 A, B). GDF15 also correlated positively with HOMA-IR (Fig. 1 C) and negatively with M-value, which reflects whole-body insulin sensitivity (but mainly driven by skeletal muscle glucose uptake) (Fig. 1 D). GDF15 further correlated positively with the Adipo-IR index, a measure of fasting adipose tissue insulin resistance (Fig. 1 E) and negatively with

Table 2 Participants' characteristics.

	OBE-CON	OBE-MASLD	OBE-MASH
Age (y)	41 (2)	44 (2)	42 (2)
Sex (female/male, N/N)	18/2	17/3	15/5
BMI (kg/m ²)	48.9 (1.5)	48.5 (1.5)	49.2 (1.7)
Waist circumference (cm)	128 (3)	133 (3)	138 (4)
Hip circumference (cm)	148 (3)	143 (3)	149 (3)
HbA1c (%)	5.4 (0.1)	5.7 (0.1)	5.6 (0.1)
Fasting glucose (mg/dL)	103 (4)	108 (3) ^a	103 (4)
Fasting insulin (mU/L)	17.4 (1.8)	20.4 (2.4)	24.4 (4.1)
Fasting glucagon (pmol/L)	9.65 (1.12)	9.64 (1.26)	10.95 (1.62)
Fasting triglycerides (mg/dL)	109 (13)	138 (7) ^a	144 (21)
Fasting NEFA (µmol/L)	712 (58)	722 (52)	668 (48)
ALT (GPT) (U/L)	25.9 (2.3)	33.8 (3.8)	41.0 (3.2)*
AST (GOT) (U/L)	22.3 (1.5)	26.2 (1.7)	28.9 (2.1)*
GGT (U/L)	24.4 (2.4)	41.5 (12.9)	34.5 (2.9)*
hsCRP (mg/dL)	0.93 (0.21)	0.82 (0.10)	0.85 (0.14)
Systolic blood pressure (mmHg)	131 (2)	135 (4)	131 (3)
Diastolic blood pressure (mmHg)	86 (2)	85 (1)	85 (2)
Type 2 diabetes (N)	2	5	3
Metformin treatment (N)	2	1	1
M-value (mg/kg/min)	2.64 (0.29)	2.60 (0.22)	2.98 (0.35)
HOMA-IR	4.53 (0.61)	5.57 (0.70)	6.37 (1.13)
Adipo-IR	72.4 (10.0)	92.5 (9.5)	81.1 (14.3)
NEFA suppression (%)	81.5 (2.6)	76.2 (3.3)	75.9 (4.0)
Serum total GDF15 (pg/mL)	616 (79)	661 (57)	635 (65)

Data are presented as mean (SEM). *p < 0.05 versus OBE-CON. Adipo-IR, adipose tissue insulin resistance index; ALT, alanine aminotransferase; AST, aspartate aminotransferase; GDF15, growth differentiation factor 15; γ GT, gamma glutamyl transferase; HbA1c, glycated hemoglobin A1c; HOMA-IR, Homeostatic Model Assessment of Insulin Resistance; hsCRP, high-sensitivity C-reactive protein; M-value, whole-body insulin-mediated glucose disposal; NEFA, non-esterified fatty acids; OBE-CON, obese humans without liver steatosis; OBE-MASLD, obese humans with metabolic dysfunction-associated steatotic liver disease; OBE-MASH, obese humans with metabolic dysfunction-associated steatohepatitis.

insulin-induced NEFA suppression, reflecting adipose tissue insulin sensitivity (Fig. 1 F). We observed no correlation between circulating GDF15 concentrations and glucagon (r = 0.246, p = 0.079), nor between GDF15 and the insulin-to-glucagon ratio (r = -0.006, p = 0.966).

3.3. Hepatic fibrosis modulates the correlation between circulating GDF15 and hepatic mitochondrial respiration

Next, we investigated if circulating GDF15 levels were related to mitochondrial respiration, which was measured ex vivo in liver, adipose tissue and skeletal muscle biopsies (Supplementary Table 1). In contrast to our hypothesis, GDF15 levels neither correlated with NADH+succinate-linked nor fatty acid substrate-linked hepatic mitochondrial respiration (Supplementary Table 2). Similarly, GDF15 did not correlate with mitochondrial respiration either in VAT and SAT or in skeletal muscle mitochondrial respiration (p > 0.05 for all tissues and respiration states) (Supplementary Table 2).

Given that GDF15 has been suggested to be higher in MASLD in the presence of fibrosis [10,11], and considering preclinical studies demonstrating anti-fibrotic properties of GDF15 [23–25], we proceeded to divide participants into those with (n=23) and without (n=37) fibrosis (Table 3).

Hepatic mitochondrial respiration linked to fatty acid oxidation (F_P: 30.2 ± 1.4 vs. 24.3 ± 1.5 , p=0.010), coupled F and NADH pathway (FN_P: 30.8 ± 1.4 vs. 25.1 ± 1.5 , p=0.007), coupled FN and succinate pathway (FNS_P: 40.8 ± 1.7 vs. 35.4 ± 1.6 , p=0.032) as well as maximal uncoupled respiration (FNS_E: 66.0 ± 2.8 vs. 55.0 ± 3.4 , p=0.016) was lower in people with hepatic fibrosis compared to those without fibrosis (Fig. 2). Interestingly, in obese humans without hepatic fibrosis, GDF15 correlated positively with coupled fatty acid oxidation-linked mitochondrial respiration (F_P; r=0.347, p=0.035), coupled F and NADH pathway-linked (FN_P; r=0.35, p=0.034) and FN and

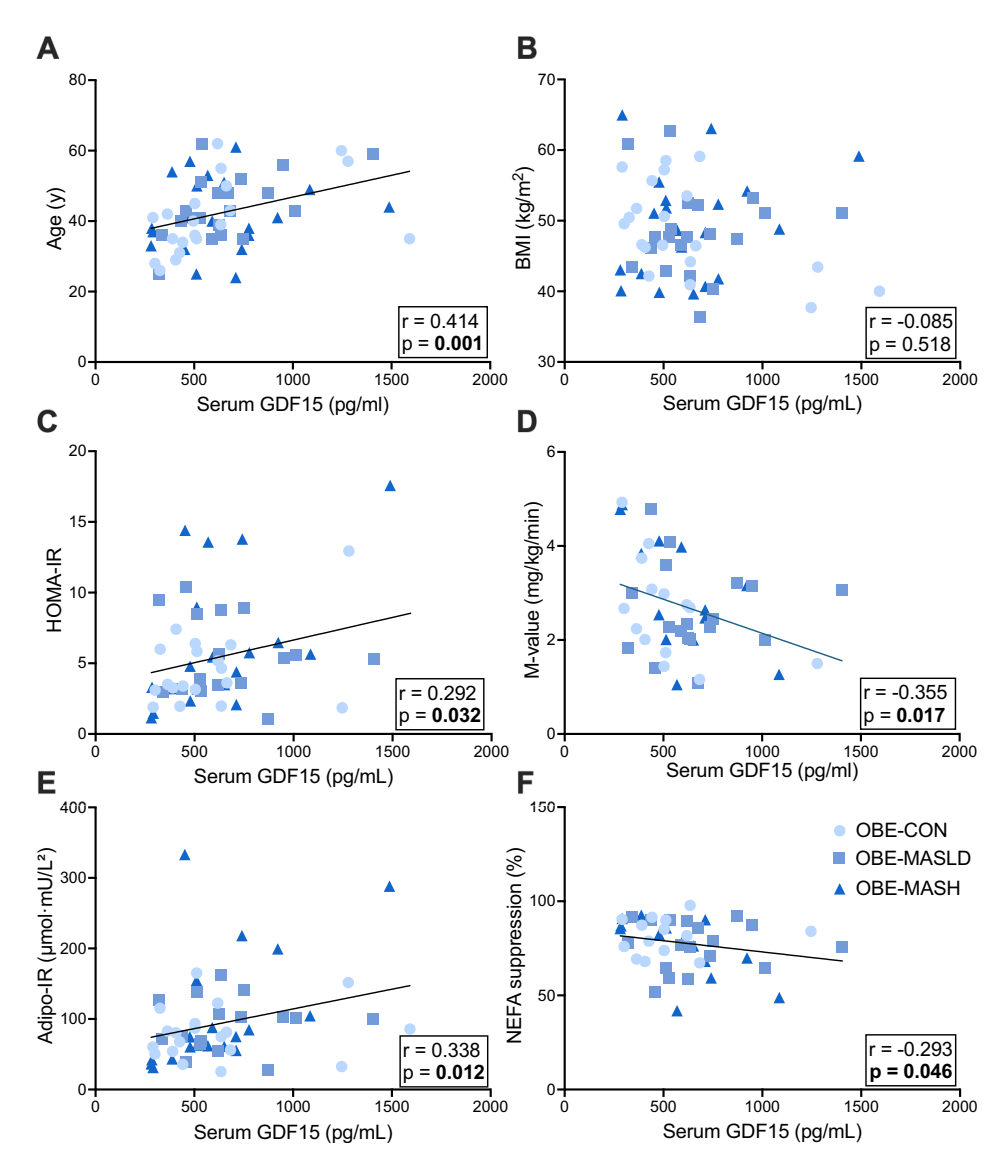


Fig. 1. Correlation of GDF15 with age, BMI, whole-body and adipose tissue insulin sensitivity.

Spearman's nonparametric correlation of GDF15 with (A) age, (B) BMI, (C) HOMA-IR, (D) insulin sensitivity (M-value), (E) adipose tissue insulin resistance index (Adipo-IR) and (F) percentage insulin-induced suppression of non-esterified fatty acid (NEFA) concentration. OBE-CON is represented by light blue circles, OBE-MASL by medium blue squares, and OBE-MASH by dark blue triangles.

Adipo-IR; adipose tissue insulin resistance index; BMI, body mass index; OBE-CON, obese participants without steatosis; GDF15, growth differentiation factor 15; HOMA-IR, Homeostatic Model Assessment of Insulin Resistance; OBE-MASH, obese participants with metabolic dysfunction-associated steatohepatitis; OBE-MASL, obese participants with steatosis; NEFA suppression (%); percentage suppression of non-esterified fatty acid concentrations. (For interpretation of the references to color in this figure legend, the reader is referred to the web version of this article.)

succinate pathway-linked (FNS_P; r=0.421, p=0.010) mitochondrial respiration (Fig. 3, A–C). In contrast, in obese humans with hepatic fibrosis, GDF15 correlated negatively with coupled fatty acid oxidationand NADH pathway-linked respiration (FN_P; r=-0.48, p=0.022) (Fig. 3, D) and tended to correlate negatively with coupled fatty acid oxidation-linked respiration (F_P; r=-0.37, p=0.083).

4. Discussion

This study shows that circulating GDF15 concentrations are positively related to whole-body and adipose tissue-specific insulin sensitivity in persons with class 3 obesity. GDF15 did neither relate to skeletal muscle nor adipose tissue mitochondrial respiration. Interestingly, hepatic fibrosis was identified as a key determinant of the relationship between circulating GDF15 and hepatic fatty acid-linked mitochondrial respiration in persons with MASLD/MASH.

As abnormal mitochondrial function may trigger the secretion of GDF15 [16,19-21,45], the main aim of our study was to examine the relationship between circulating GDF15 levels and tissue-specific mitochondrial respiration. A strength of our study is that we were able to use high-resolution respirometry to assess mitochondrial respiration in tissue samples of not only skeletal muscle and subcutaneous adipose tissue, but also visceral adipose tissue as well as liver of humans featuring obesity with and without MASLD. For muscle and adipose tissue, we did not find any correlation between GDF15 and mitochondrial respiration. Regarding hepatic mitochondrial respiration, we previously demonstrated that mitochondrial oxidative capacity is higher in obese humans without MASH as compared to lean humans, reflecting an adaptation (mitochondrial plasticity), which is lost in humans with MASH and/or with obesity or type 2 diabetes [2,14]. Of note, despite no significant difference in GDF15 levels between the groups and no correlation between GDF15 and hepatic mitochondrial respiration across

Table 3Characteristics of participants stratified by fibrosis status.

	No fibrosis ($n = 37$)	Fibrosis ($n = 23$)
Age (y)	41 (2)	44 (2)
Sex (female/male, N/N)	33/4	17/6
BMI (kg/m ²)	49.1 (1.2)	48.5 (1.4)
Waist circumference (cm)	133 (3)	134 (3)
Hip circumference (cm)	146 (2)	148 (3)
HbA1c (%)	5.6 (0.1)	5.6 (0.1)
Fasting glucose (mg/dL)	103 (3)	107 (4)
Fasting insulin (mU/L)	19.1 (2.2)	23.2 (2.8)
Fasting glucagon (pmol/L)	10.28 (0.95)	9.83 (1.33)
Fasting triglycerides (mg/dL)	135 (10)	128 (18)
Fasting NEFA (µmol/L)	707 (45)	679 (41)
ALT (GPT) (U/L)	29.8 (2.3)	39.7 (3.3)*
AST (GOT) (U/L)	23.4 (1.2)	29.7 (1.8)*
GGT (U/L)	34.5 (7.1)	31.8 (2.9)
hsCRP (mg/dL)	0.91 (0.13)	0.80 (0.11)
Systolic blood pressure (mmHg)	133 (2)	132 (2)
Diastolic blood pressure (mmHg)	86 (1)	83 (2)
Type 2 diabetes (N)	6	4
Metformin treatment (N)	4	0
M-value (mg/kg/min)	2.75 (0.21)	2.89 (0.27)
HOMA-IR	4.49 (0.51)	5.18 (0.74)
Adipo-IR	78.7 (7.7)	85.7 (10.2)
NEFA suppression (%)	80.3 (2.4)	73.8 (3.4)
Serum total GDF15 (pg/mL)	640 (53)	633 (53)

Data are presented as mean (SEM). $^*p < 0.05$ versus no fibrosis. Adipo-IR, adipose tissue insulin resistance index; ALT, alanine aminotransferase; AST, aspartate aminotransferase; GDF15, growth differentiation factor 15; GGT, gamma glutamyl transferase; HbA1c, glycated hemoglobin A1c; HOMA-IR, Homeostatic Model Assessment of Insulin Resistance; hsCRP, high-sensitivity C-reactive protein; M-value, whole-body insulin-mediated glucose disposal; NEFA, non-esterified fatty acids.

the whole cohort, we detected that the relationship between hepatic mitochondrial respiration and GDF15 is influenced by the presence of hepatic fibrosis. Specifically, GDF15 levels correlated positively with hepatic fatty acid-related mitochondrial respiration in individuals without fibrosis, but negatively in individuals with fibrosis. These findings raise the possibility that GDF15 might contribute to the

maintenance of mitochondrial β-oxidation in obesity and early stages of MASLD. In humans with obesity and hepatic fibrosis, the loss of mitochondrial adaptation mirrored by impaired hepatic oxidative capacity may be associated with increased GDF15 levels, potentially reflecting an attempt to counteract the negative effect of fibrosis on mitochondrial function. Future studies are needed to further test these hypothesis, however earlier studies have also proposed such a role of GDF15 as a mitokine [26]. In this context, loss of mitochondrial β-oxidation through liver-specific deletion of carnitine palmitoyltransferase 2 (Cpt2) in highfat diet-fed mice was shown to increase both hepatic GDF15 mRNA expression and serum GDF15 [19]. Additionally, mice with dynamin related protein 1 (Drp1) knockdown, a key mitochondrial fission protein, exhibited lower mitochondrial respiration accompanied by upregulated hepatic GDF15 mRNA expression through activation of the Activating Transcription Factor 4 (ATF4)-controlled integrated stress response (ISR) and increased serum GDF15 levels [20]. Furthermore, future studies are needed to investigate whether GDF15 administration to fibrotic livers reverses the downregulation of hepatic mitochondrial oxidative capacity and thereby even improves liver histology, lipid metabolism and insulin resistance. Improvement of mitochondrial function underlies the mechanism of action of resmetirom, the only currently approved drug from MASH with fibrosis [46], as well as of the drug class of mitochondrial uncouplers [47]. Indeed, GDF15 has been already discussed as a promising therapeutic target for metabolic diseases [26] including MASLD/MASH [13,17].

Another unique aspect of our study is the availability of skeletal muscle, SAT, VAT and liver samples in humans with and without MASLD for the assessment of mitochondrial OXPHOS. We found no differences in GDF15 levels across humans with grade 3 obesity without MASLD, with MASLD and with MASH, with similar age, sex and BMI, which is in contrast with previous studies showing elevated GDF15 in MASLD and MASH [8,10,12]. However, we confirm the earlier reported strong positive correlation between age and circulating GDF15 levels [6]. Of note, most [8,10,12], but not all [9,11], previous studies showing increases in circulating GDF15 in MASLD investigated participants with MASH who were overall 5–10-years older [8,10,12], and/or with a higher prevalence of type 2 diabetes (>40 % vs.16.7 %) [10,12] as

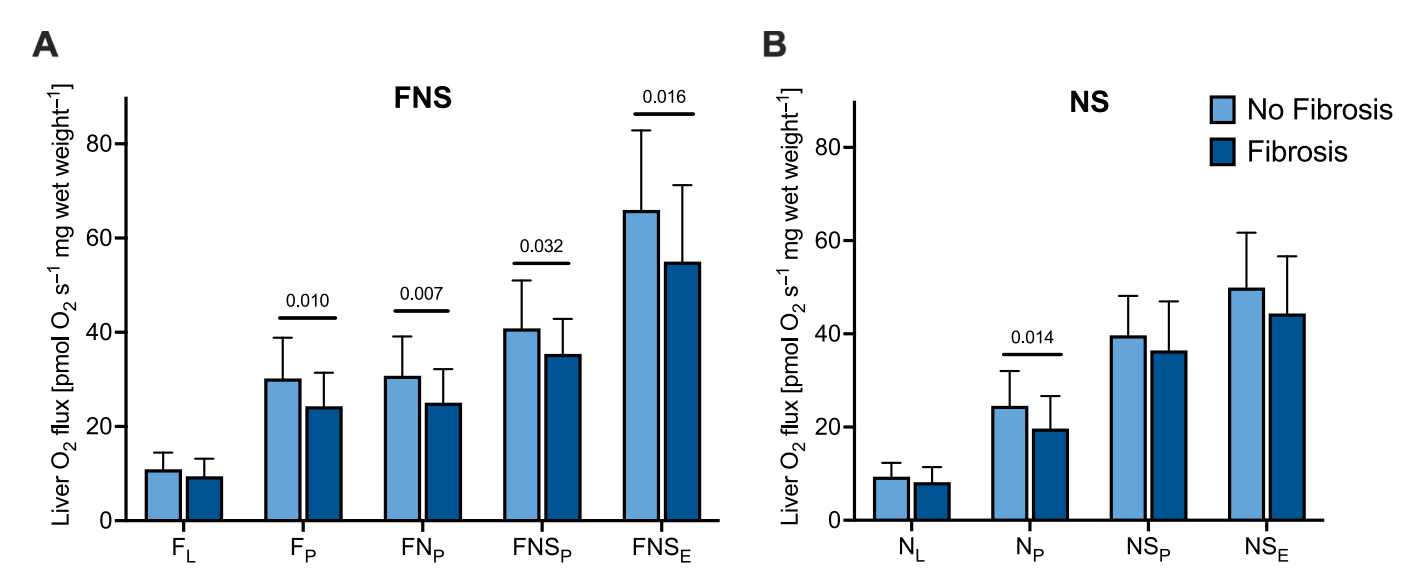


Fig. 2. Hepatic fatty acid oxidation- and NADH + succinate-linked respiration rates in participants with obesity stratified by presence of hepatic fibrosis. (A) Hepatic fatty acid and- NADH -and succinate-linked mitochondrial respiration and (B) NADH and succinate-linked mitochondrial respiration in participants with obesity stratified by presence or absence of fibrosis. Data are presented as means \pm SEM. Between-group differences were calculated using Student's t-test or nonparametric Mann-Whitney-U test, based on data distribution. Statistical significance was set at p < 0.05.

 $F_{L_{P}}$ leak respiration (L) with electron input through the F pathway; $F_{P_{P}}$, OXPHOS capacity (P) with electron input through the F pathway; $F_{N_{P}}$, P with electron input through the F, N, and S pathways combined; $F_{N_{P}}$, P with electron input through the F, N, and S pathways combined; $F_{N_{P}}$, P with electron input through the F, N, and S pathways combined; $F_{N_{P}}$, P with electron input through the N pathway; $F_{N_{P}}$, P with electron input through the N and S pathways combined; $F_{N_{P}}$, P with electron input through the N and S pathways combined; $F_{N_{P}}$, P with electron input through the N and S pathways combined; $F_{N_{P}}$, P with electron input through the N and S pathways combined; $F_{N_{P}}$, P with electron input through the N and S pathways combined; $F_{N_{P}}$, P with electron input through the N and S pathways combined; $F_{N_{P}}$, P with electron input through the N and S pathways combined; $F_{N_{P}}$, P with electron input through the N and S pathways combined; $F_{N_{P}}$, P with electron input through the N and S pathways combined; $F_{N_{P}}$, P with electron input through the N and S pathways combined; $F_{N_{P}}$, P with electron input through the N and S pathways combined; $F_{N_{P}}$, P with electron input through the N and S pathways combined; $F_{N_{P}}$, P with electron input through the N and S pathways combined; $F_{N_{P}}$, P with electron input through the N and S pathways combined; $F_{N_{P}}$, P with electron input through the N and S pathways combined; $F_{N_{P}}$, P with electron input through the N and S pathways combined; $F_{N_{P}}$, P with electron input through the N and S pathways combined; $F_{N_{P}}$, P with electron input through the N and S pathways combined; $F_{N_{P}}$, P with electron input through the N and S pathways combined; $F_{N_{P}}$, P with electron input through the N and S pathways combined; $F_{N_{P}}$, P with electron input through the N and S pathways combined; $F_{N_{P}}$, P with electron input through the

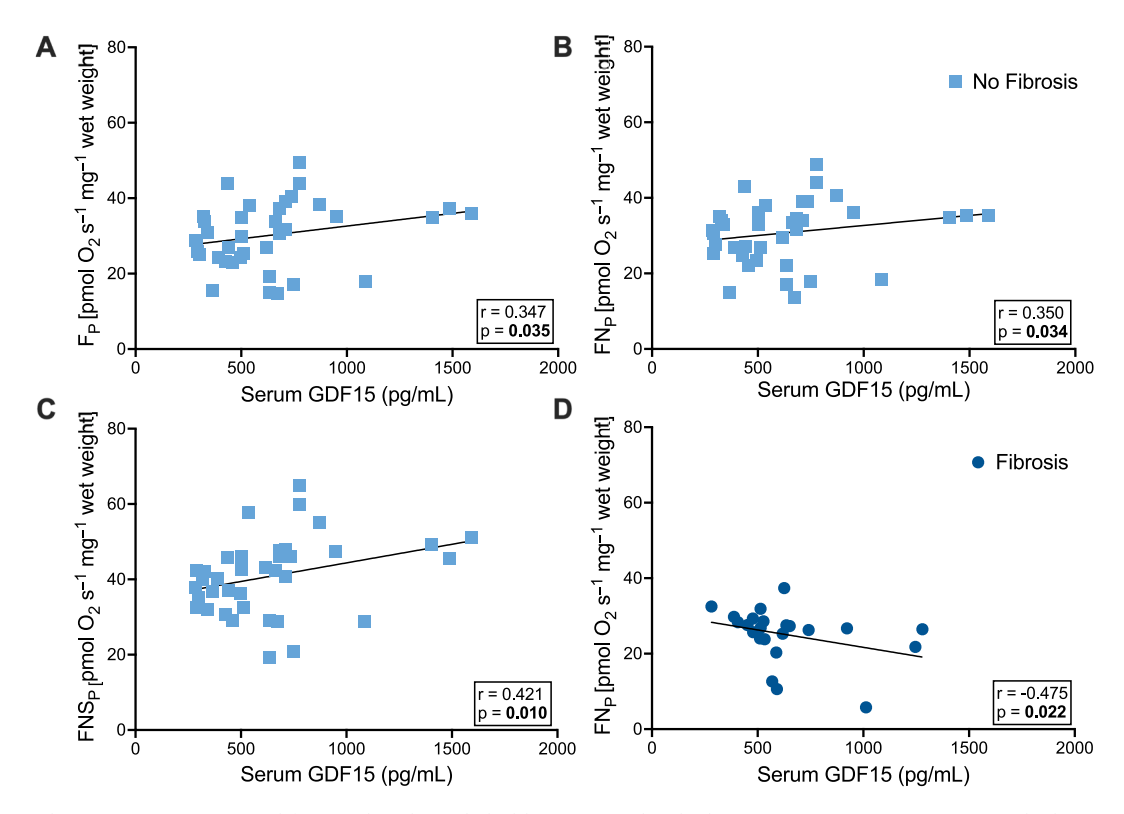


Fig. 3. Correlations between serum GDF15 and fatty acid oxidation-linked hepatic mitochondrial respiration rates in participants with obesity with and without hepatic fibrosis.

Spearman's nonparametric correlations between serum GDF15 and (A) hepatic OXPHOS capacity with electron input through the fatty acid oxidation (F) pathway (F_P), (B) P with electron input through the F and NADH (N) pathways combined (FN_P), and (C) P with electron input through the F, N, and succinate (S) pathways combined (FNS_P), in participants with no fibrosis. (D) Spearman's nonparametric correlations between serum GDF15 and hepatic P with electron input through the F and N pathways combined (FN_P), in participants with fibrosis. Individuals without fibrosis are shown as medium blue squares and individuals with fibrosis are shown as dark blue circles. Significance was set at p < 0.05.

GDF15, growth differentiation factor; F_P , OXPHOS capacity (P) with electron input through the F pathway; F_{NP} , P with electron input through the F and N pathways combined; F_{NP} , P with electron input through the F, N, and S pathways combined. (For interpretation of the references to color in this figure legend, the reader is referred to the web version of this article.)

compared to our study. Finally, the participants of the BARIA-DDZ cohort exhibited relatively mild histological features of MASH. This underlines a specific role of GDF15 during the early development of metabolic disease and MASLD/MASH.

The present study reveals an association between hepatic mitochondrial respiration in MASLD and serum GDF15 levels. However, since we only measured circulating GDF15 without assessing tissuespecific expression, we cannot determine the tissue contribution to circulating GDF15 in obesity and MASLD. This limitation, combined with the cross-sectional design, precludes conclusions about the sources of circulating GDF15 or its mechanistic links to mitochondrial function in different tissues. Recent evidence has suggested that in the early stages of obesity and T2D, visceral adipose tissue is the main contributing tissue to circulating GDF15 [5]. However, with progression to MASH, the liver may become the predominant source, and GDF15 mRNA expression was associated with hepatic fibrosis [5]. However, in another recent study by Werge et al. [12], hepatic GDF15 mRNA expression correlated with steatosis grade, but not with fibrosis stage. Of note, while preclinical studies showed that GDF15 is secreted from skeletal muscle in response to exercise/stress, human studies failed to confirm these results, and point towards liver and splanchnic organs as the main contributors to circulating GDF15 levels [48–50]. Further studies are required to determine tissue-specific GDF15 mRNA expression in relation to mitochondrial function and circulating GDF15 levels in obesity and MASLD.

Using the gold-standard hyperinsulinemic-euglycemic clamp, the present study also validated the positive relationship of GDF15 with

surrogates of insulin resistance such as the HOMA-IR, OGTT-derived insulin sensitivity or fasting C-peptide [6,7]. Specifically, we now detected a similar correlation of GDF15 with adipose-tissue insulin sensitivity at fasting (Adipo-IR) and under clamp conditions (NEFA suppression). Recent human studies further suggest that glucagon increases circulating GDF15 levels in an insulin-dependent manner [31,48], particularly in MASLD [31]. However, here we did not find a relation between glucagon and/or glucagon:insulin ratio with GDF15 levels. These data may serve to support the concept of compensatory GDF15 secretion to combat insulin resistance. This concept is based on the improvement in glucose homeostasis and insulin sensitivity upon recombinant GDF15 treatment or GDF15 overexpression [51], which is not only related to its appetite-lowering effects [2,51] but also occurring independently of weight loss in preclinical studies [17,18].

Some strengths and weaknesses need to be considered in the context of our study. The present study benefits from the investigation of the comprehensively phenotyped BARIA-DDZ cohort comprising liver histology, in vivo assessment of insulin sensitivity and ex vivo measurements of various features of mitochondrial function in different tissues. Nevertheless, certain limitations need to be mentioned. Due to ethical considerations, liver biopsies were not available from a lean control group, which limits the generalizability of our findings. Also, the small spatial resolution and the histological scoring of liver biopsies might not capture any heterogenous distribution of histological features across the liver [38]. The characteristics of the study population, i.e. class 3 obesity and the overall mild liver disease, prevent from extrapolation to people with severe MASH with advanced fibrosis. Finally, the cross-sectional

design does not allow conclusions about causality of the observed relationships.

In conclusion, circulating GDF15 levels are positively related to hepatic fatty acid-linked mitochondrial respiration in humans with class 3 obesity without hepatic fibrosis, suggesting a positive relationship between GDF15 and mitochondrial respiration in early stages of obesity-related MASLD before hepatic fibrosis develops. However, in people with hepatic fibrosis, hepatic mitochondrial respiration was impaired and circulating GDF15 levels were negatively related to hepatic mitochondrial respiration. Further research is required to determine if and how GDF15 influences hepatic mitochondrial respiration depending on fibrosis, and conversely, how fibrosis might impact hepatic GDF15 secretion by altering mitochondrial function.

CRediT authorship contribution statement

Anna Giannakogeorgou: Writing - original draft, Visualization, Investigation, Data curation. Sabine Kahl: Writing – review & editing, Resources, Project administration, Investigation, Data curation. Cesare Granata: Writing - review & editing, Investigation. Geronimo Heilmann: Writing – review & editing, Investigation. Lucia Mastrototaro: Writing – review & editing, Investigation, **Bedair Dewidar**: Writing – review & editing, Investigation. Pavel Bobrov: Writing - review & editing, Formal analysis. Irene Esposito: Writing - review & editing, Investigation. Aslihan Yavas: Writing – review & editing, Investigation. Sandra Trenkamp: Writing - review & editing, Investigation. Frank A. Granderath: Writing - review & editing, Investigation. Matthias Schlensak: Writing - review & editing, Investigation. Christos S. Mantzoros: Writing - review & editing, Supervision, Resources, Conceptualization. Michael Roden: Writing - review & editing, Supervision, Resources, Project administration, Methodology, Funding acquisition, Conceptualization. Patrick Schrauwen: Writing - review & editing, Supervision, Project administration, Methodology, Conceptualization.

Funding sources

The research of the German Diabetes Center (DDZ) is funded by the German Federal Ministry of Health and the Ministry of Culture and Science of the state of Northrhine-Westphalia and the German Federal Ministry of Education and Research (to the German Center for Diabetes Research, DZD) and the Schmutzler-Stiftung. The research of M.R. is further supported by grants from the German Research Foundation (DFG) (GRK 2576) and the European Community (HORIZON-HLTH-2022-STAYHLTH-02-01: Panel A) to the INTERCEPT-T2D consortium. The research of S.K. is further supported by grants from the German Diabetes Association (Deutsche Diabetes Gesellschaft (DDG); Menarini Projektförderung; Hans-Christian-Hagedorn-Projektförderung).

Declaration of competing interest

The authors declare the following financial interests/personal relationships which may be considered as potential competing interests: Michael Roden reports a relationship with AstraZeneca that includes: board membership. Michael Roden reports a relationship with Boehringer Ingelheim GmbH that includes: board membership and funding grants. Michael Roden reports a relationship with Echosens SA that includes: board membership. Michael Roden reports a relationship with Madrigal Pharmaceuticals Inc. that includes: board membership. Michael Roden reports a relationship with Eli Lilly and Company that includes: board membership. Michael Roden reports a relationship with MSD Merck Sharp & Dohme AG that includes: board membership. Michael Roden reports a relationship with Novo Nordisk that includes: board membership and funding grants. Michael Roden reports a relationship with Target RWE that includes: board membership. Michael Roden reports a relationship with Danone Nutricia Research that

includes: funding grants. Christos S Mantzoros reports a relationship with Merck & Co Inc. that includes: funding grants and non-financial support. Christos S Mantzoros reports a relationship with Massachusetts Life Sciences Center that includes: funding grants. Christos S Mantzoros reports a relationship with Boehringer Ingelheim Corp USA that includes: funding grants and non-financial support. Christos S Mantzoros reports a relationship with Esperion Therapeutics Inc. that includes: funding grants. Christos S Mantzoros reports a relationship with Ansh Labs LLC that includes: consulting or advisory and funding grants. Christos S Mantzoros reports a relationship with Labcorp Drug Development Inc. that includes: funding grants. Christos S Mantzoros reports a relationship with Nestle that includes: consulting or advisory. Christos S Mantzoros reports a relationship with Olympus America Inc. that includes: consulting or advisory. Christos S Mantzoros reports a relationship with Genfit SA that includes: consulting or advisory. Christos S Mantzoros reports a relationship with Lumos Pharma that includes: consulting or advisory. Christos S Mantzoros reports a relationship with Novo Nordisk that includes: consulting or advisory. Christos S Mantzoros reports a relationship with Amgen Inc. that includes: consulting or advisory. Christos S Mantzoros reports a relationship with Corcept Therapeutics Inc. that includes: consulting or advisory. Christos S Mantzoros reports a relationship with Intercept Pharmaceuticals Inc. that includes: consulting or advisory. Christos S Mantzoros reports a relationship with 89bio Ltd. that includes: consulting or advisory. Christos S Mantzoros reports a relationship with Madrigal Pharmaceuticals Inc. that includes: consulting or advisory. Christos S Mantzoros reports a relationship with Aligos Therapeutics Inc. that includes: consulting or advisory. Christos S Mantzoros reports a relationship with Esperion Therapeutics Inc. that includes: consulting or advisory and non-financial support. Christos S Mantzoros reports a relationship with Biodexa Pharmaceuticals PLC that includes: consulting or advisory. Christos S Mantzoros reports a relationship with Regeneron Pharmaceuticals Inc. that includes: consulting or advisory. Christos S Mantzoros reports a relationship with UptoDate Inc. that includes: speaking and lecture fees and travel reimbursement. Travel support and fees from reports a relationship with The Metabolic Institute of America that includes: speaking and lecture fees and travel reimbursement. Christos S Mantzoros reports a relationship with Elsevier that includes: speaking and lecture fees and travel reimbursement. Christos S Mantzoros reports a relationship with Cardio Metabolic Health Conference that includes: speaking and lecture fees and travel reimbursement. Sabine Kahl reports a relationship with German Diabetes Association (DDG) that includes: funding grants. The research of the German Diabetes Center (DDZ) is funded by the German Federal Ministry of Health and the Ministry of Culture and Science of the state of Northrhine-Westphalia and the German Federal Ministry of Education and Research (to the German Center for Diabetes Research). If there are other authors, they declare that they have no known competing financial interests or personal relationships that could have appeared to influence the work reported in this paper.

Acknowledgements

Personal thanks. We would like to thank all study participants from the BARIA-DDZ study. We acknowledge the help of Fariba Zivehe, Olga Dürrschmidt and Alexandra Stein for their invaluable contribution, technical expertise and outstanding support in the organizational and laboratory aspects of this project. We thank Georgia Xourafa and Maximilian Huttasch for their dedicated collaboration in conducting the study visits and clinical experiments. Additionally, we would like to thank Anita Shokouhmehr for managing and maintaining the database as well as Jessica Oberhäuser, Michelle Reina Do Fundo and Jan-Marc Leonhard for their excellent technical assistance.

Appendix A. Supplementary data

Supplementary data to this article can be found online at https://doi.org/10.1016/j.metabol.2025.156391.

References

- Wang D, Day EA, Townsend LK, Djordjevic D, Jørgensen SB, Steinberg GR. GDF15: emerging biology and therapeutic applications for obesity and cardiometabolic disease. Nat Rev Endocrinol 2021;17:592–607. https://doi.org/10.1038/s41574-021.00579.7
- [2] Xourafa G, Korbmacher M, Roden M. Inter-organ crosstalk during development and progression of type 2 diabetes mellitus. Nat Rev Endocrinol 2024;20:27–49. https://doi.org/10.1038/s41574-023-00898-1.
- [3] Lockhart SM, Saudek V, O'Rahilly S. GDF15: a hormone conveying somatic distress to the brain. Endocr Rev 2020;41:bnaa007. https://doi.org/10.1210/endrev/ bnaa007
- [4] Dostálová I, Roubíček T, Bártlová M, Mráz M, Lacinová Z, Haluzíková D, et al. Increased serum concentrations of macrophage inhibitory cytokine-1 in patients with obesity and type 2 diabetes mellitus: the influence of very low calorie diet. Eur J Endocrinol 2009;161:397–404. https://doi.org/10.1530/EJE-09-0417.
- [5] L'homme L, Sermikli BP, Haas JT, Fleury S, Quemener S, Guinot V, et al. Adipose tissue macrophage infiltration and hepatocyte stress increase GDF-15 throughout development of obesity to MASH. Nat Commun 2024;15:7173. https://doi.org/ 10.1038/s41467-024-51078-2.
- [6] Kleinert M, Bojsen-Møller KN, Jørgensen NB, Svane MS, Martinussen C, Kiens B, et al. Effect of bariatric surgery on plasma GDF15 in humans. Am J Physiol-Endocrinol Metab 2019;316:E615–21. https://doi.org/10.1152/aipendo.00010.2019
- [7] Hong JH, Chung HK, Park HY, Joung K-H, Lee JH, Jung JG, et al. GDF15 is a novel biomarker for impaired fasting glucose. Diabetes Metab J 2014;38:472. https:// doi.org/10.4093/dmj.2014.38.6.472.
- [8] Boutari C, Stefanakis K, Simati S, Guatibonza-García V, Valenzuela-Vallejo L, Anastasiou IA, et al. Circulating total and H-specific GDF15 levels are elevated in subjects with MASLD but not in hyperlipidemic but otherwise metabolically healthy subjects with obesity. Cardiovasc Diabetol 2024;23:174. https://doi.org/ 10.1186/c12023-024-02564-5
- [9] Chang JS, Ahn J-H, Kim MY, Park K-S. Elevated serum growth differentiation factor 15 and decorin predict the fibrotic progression of metabolic dysfunction-associated steatotic liver disease. Sci Rep 2024;14:27527. https://doi.org/10.1038/s41598-024-77719-6
- [10] Valenzuela-Vallejo L, Chrysafi P, Kouvari M, Guatibonza-Garcia V, Mylonakis SC, Katsarou A, et al. Circulating hormones in biopsy-proven steatotic liver disease and steatohepatitis: a multicenter observational Study. Metabolism 2023;148:155694. https://doi.org/10.1016/j.metabol.2023.155694.
- [11] Koo BK, Um SH, Seo DS, Joo SK, Bae JM, Park JH, et al. Growth differentiation factor 15 predicts advanced fibrosis in biopsy-proven non-alcoholic fatty liver disease. Liver Int 2018;38:695–705. https://doi.org/10.1111/liv.13587.
- [12] Werge MP, Grandt J, Thing M, Hetland LE, Rashu EB, Jensen AH, et al. Circulating and hepatic levels of growth differentiation factor 15 in patients with metabolic dysfunction-associated steatotic liver disease. Hepatol Res 2024:hepr.14148. https://doi.org/10.1111/hepr.14148.
- [13] Patel S, Haider A, Alvarez-Guaita A, Bidault G, El-Sayed Moustafa JS, Guiu-Jurado E, et al. Combined genetic deletion of GDF15 and FGF21 has modest effects on body weight, hepatic steatosis and insulin resistance in high fat fed mice. Mol Metab 2022;65:101589. https://doi.org/10.1016/i.molmet.2022.101589.
- [14] Fromenty B, Roden M. Mitochondrial alterations in fatty liver diseases. J Hepatol 2023;78:415–29. https://doi.org/10.1016/j.jhep.2022.09.020.
- [15] Georgiev A, Granata C, Roden M. The role of mitochondria in the pathophysiology and treatment of common metabolic diseases in humans. Am J Physiol-Cell Physiol 2022;322:C1248–59. https://doi.org/10.1152/ajpcell.00035.2022.
- [16] Ost M, Igual Gil C, Coleman V, Keipert S, Efstathiou S, Vidic V, et al. Muscle-derived GDF15 drives diurnal anorexia and systemic metabolic remodeling during mitochondrial stress. EMBO Rep 2020;21:e48804. https://doi.org/10.15252/embr.201948804.
- [17] Sjøberg KA, Sigvardsen CM, Alvarado-Diaz A, Andersen NR, Larance M, Seeley RJ, et al. GDF15 increases insulin action in the liver and adipose tissue via a β-adrenergic receptor-mediated mechanism. Cell Metab 2023;35:1327–1340.e5. https://doi.org/10.1016/j.cmet.2023.06.016.
- [18] Wang D, Townsend LK, DesOrmeaux GJ, Frangos SM, Batchuluun B, Dumont L, et al. GDF15 promotes weight loss by enhancing energy expenditure in muscle. Nature 2023;619:143–50. https://doi.org/10.1038/s41586-023-06249-4.
- [19] Lee J, Choi J, Selen Alpergin ES, Zhao L, Hartung T, Scafidi S, et al. Loss of hepatic mitochondrial long-chain fatty acid oxidation confers resistance to diet-induced obesity and glucose intolerance. Cell Rep 2017;20:655–67. https://doi.org/ 10.1016/j.celrep.2017.06.080.
- [20] Steffen J, Ngo J, Wang S-P, Williams K, Kramer HF, Ho G, et al. The mitochondrial fission protein Drp1 in liver is required to mitigate NASH and prevents the activation of the mitochondrial ISR. Mol Metab 2022;64:101566. https://doi.org/ 10.1016/j.molmet.2022.101566.
- [21] Choi MJ, Jung S-B, Lee SE, Kang SG, Lee JH, Ryu MJ, et al. An adipocyte-specific defect in oxidative phosphorylation increases systemic energy expenditure and protects against diet-induced obesity in mouse models. Diabetologia 2020;63: 837–52. https://doi.org/10.1007/s00125-019-05082-7.

- [22] Chen J, Kastroll J, Bello FM, Pangburn MM, Murali A, Smith PM, et al. Skeletal muscle mitochondrial dysfunction is associated with increased Gdf15 expression and circulating GDF15 levels in aged mice. Sci Rep 2025;15:8101. https://doi.org. 10.1038/s41598-025-92572-x
- [23] Li X, Huai Q, Zhu C, Zhang X, Xu W, Dai H, et al. GDF15 ameliorates liver fibrosis by metabolic reprogramming of macrophages to acquire anti-inflammatory properties. Cell Mol Gastroenterol Hepatol 2023;16:711–34. https://doi.org/ 10.1016/j.jcmgh.2023.07.009.
- [24] Jurado-Aguilar J, Barroso E, Bernard M, Zhang M, Peyman M, Rada P, et al. GDF15 activates AMPK and inhibits gluconeogenesis and fibrosis in the liver by attenuating the TGF-β1/SMAD3 pathway. Metabolism 2024;152:155772. https://doi.org/10.1016/j.metabol.2023.155772.
- [25] Kim KH, Kim SH, Han DH, Jo YS, Lee Y, Lee M-S. Growth differentiation factor 15 ameliorates nonalcoholic steatohepatitis and related metabolic disorders in mice. Sci Rep 2018;8:6789. https://doi.org/10.1038/s41598-018-25098-0.
- [26] Sigvardsen CM, Richter MM, Engelbeen S, Kleinert M, Richter EA. GDF15 is still a mystery hormone. Trends Endocrinol Metab 2024:S1043276024002546. https://doi.org/10.1016/j.tem.2024.09.002.
- [27] De Zegher F, Díaz M, Villarroya J, Cairó M, López-Bermejo A, Villarroya F, et al. The relative deficit of GDF15 in adolescent girls with PCOS can be changed into an abundance that reduces liver fat. Sci Rep 2021;11. https://doi.org/10.1038/s41598-021-86317-9.
- [28] Myojin Y, Hikita H, Tahata Y, Doi A, Kato S, Sasaki Y, et al. Serum growth differentiation factor 15 predicts hepatocellular carcinoma occurrence after hepatitis C virus elimination. Aliment Pharmacol Ther 2022;55:422–33. https:// doi.org/10.1111/apt.16691.
- [29] Monzo L, Kobayashi M, Ferreira JP, Lamiral Z, Delles C, Clark AL, et al. Echocardiographic and biomarker characteristics in diabetes, coronary artery disease or both: insights from HOMAGE trial. Cardiovasc Diabetol 2025;24. https://doi.org/10.1186/s12933-025-02609-8.
- [30] Xiao Q-A, He Q, Zeng J, Xia X. GDF-15, a future therapeutic target of glucolipid metabolic disorders and cardiovascular disease. Biomed Pharmacother 2022;146: 112582. https://doi.org/10.1016/j.biopha.2021.112582.
- [31] Richter MM, Kemp IM, Heebøll S, Winther-Sørensen M, Kjeldsen SAS, Jensen NJ, et al. Glucagon augments the secretion of FGF21 and GDF15 in MASLD by indirect mechanisms. Metabolism 2024;156:155915. https://doi.org/10.1016/j.metabol.2024.155915.
- [32] Kahl S, Straßburger K, Pacini G, Trinks N, Pafili K, Mastrototaro L, et al. Dysglycemia and liver lipid content determine the relationship of insulin resistance with hepatic OXPHOS capacity in obesity. J Hepatol 2025;82:417–26. https://doi. org/10.1016/j.jhep.2024.08.012.
- [33] Gancheva S, Ouni M, Jelenik T, Koliaki C, Szendroedi J, Toledo FGS, et al. Dynamic changes of muscle insulin sensitivity after metabolic surgery. Nat Commun 2019; 10:4179. https://doi.org/10.1038/s41467-019-12081-0.
- [34] Gancheva S, Kahl S, Pesta D, Mastrototaro L, Dewidar B, Strassburger K, et al. Impaired hepatic mitochondrial capacity in nonalcoholic steatohepatitis associated with type 2 diabetes. Diabetes Care 2022;45:928–37. https://doi.org/10.2337/ dc21-1758
- [35] Gancheva S, Kahl S, Herder C, Strassburger K, Sarabhai T, Pafili K, et al. Metabolic surgery-induced changes of the growth hormone system relate to improved adipose tissue function. Int J Obes (Lond) 2023;47:505–11. https://doi.org/10.1038/ s41366-023-01292-7.
- [36] Bódis K, Kahl S, Simon M-C, Zhou Z, Sell H, Knebel B, et al. Reduced expression of stearoyl-CoA desaturase-1, but not free fatty acid receptor 2 or 4 in subcutaneous adipose tissue of patients with newly diagnosed type 2 diabetes mellitus. Nutr Diabetes 2018;8:49. https://doi.org/10.1038/s41387-018-0054-9.
- [37] Koliaki C, Szendroedi J, Kaul K, Jelenik T, Nowotny P, Jankowiak F, et al. Adaptation of hepatic mitochondrial function in humans with non-alcoholic fatty liver is lost in steatohepatitis. Cell Metab 2015;21:739–46. https://doi.org/ 10.1016/j.cmet.2015.04.004.
- [38] Bedossa P, Poitou C, Veyrie N, Bouillot J-L, Basdevant A, Paradis V, et al. Histopathological algorithm and scoring system for evaluation of liver lesions in morbidly obese patients. Hepatology 2012;56:1751–9. https://doi.org/10.1002/ hep.25889.
- [39] Tacke F, Horn P, Wai-Sun Wong V, Ratziu V, Bugianesi E, Francque S, et al. EASL–EASD–EASO Clinical Practice Guidelines on the management of metabolic dysfunction-associated steatotic liver disease (MASLD). J Hepatol 2024;81: 492–542. https://doi.org/10.1016/j.jhep.2024.04.031.
- [40] Kleiner DE, Brunt EM, Van Natta M, Behling C, Contos MJ, Cummings OW, et al. Design and validation of a histological scoring system for nonalcoholic fatty liver disease†. Hepatology 2005;41:1313–21. https://doi.org/10.1002/hep.20701.
- [41] Pafili K, Kahl S, Mastrototaro L, Strassburger K, Pesta D, Herder C, et al. Mitochondrial respiration is decreased in visceral but not subcutaneous adipose tissue in obese individuals with fatty liver disease. J Hepatol 2022;77:1504–14. https://doi.org/10.1016/j.jhep.2022.08.010.
- [42] Heilmann G, Trenkamp S, Möser C, Bombrich M, Schön M, Yurchenko I, et al. Precise glucose measurement in sodium fluoride-citrate plasma affects estimates of prevalence in diabetes and prediabetes. Clinical Chemistry and Laboratory Medicine (CCLM) 2024;62:762–9. https://doi.org/10.1515/cclm-2023-0770.
- [43] Granata C, Caruana NJ, Botella J, Jamnick NA, Huynh K, Kuang J, et al. Highintensity training induces non-stoichiometric changes in the mitochondrial proteome of human skeletal muscle without reorganisation of respiratory chain content. Nat Commun 2021;12:7056. https://doi.org/10.1038/s41467-021-27153-3.
- [44] Gnaiger E. Mitochondrial Pathways and Respiratory Control: An Introduction to OXPHOS Analysis. 5th ed. 2020. https://doi.org/10.26124/BEC:2020-0002.

- [45] Lee H-Y, Nga HT, Tian J, Yi H-S. Mitochondrial metabolic signatures in hepatocellular carcinoma. Cells 2021;10:1901. https://doi.org/10.3390/ cells10081901
- [46] Harrison SA, Bedossa P, Guy CD, Schattenberg JM, Loomba R, Taub R, et al. A phase 3, randomized, controlled trial of resmetirom in NASH with liver fibrosis. N Engl J Med 2024;390:497–509. https://doi.org/10.1056/NEJMoa2309000.
- [47] Mastrototaro L, Roden M. Insulin resistance and insulin sensitizing agents. Metabolism 2021;125:154892. https://doi.org/10.1016/j.metabol.2021.154892.
- [48] Plomgaard P, Hansen JS, Townsend LK, Gudiksen A, Secher NH, Clemmesen JO, et al. GDF15 is an exercise-induced hepatokine regulated by glucagon and insulin in humans. Front Endocrinol 2022;13:1037948. https://doi.org/10.3389/fendo.2022.1037948.
- [49] Laurens C, Parmar A, Murphy E, Carper D, Lair B, Maes P, et al. Growth and differentiation factor 15 is secreted by skeletal muscle during exercise and promotes lipolysis in humans. JCI Insight 2020;5:e131870. https://doi.org/ 10.1172/jci.insight.131870.
- [50] Kleinert M, Clemmensen C, Sjøberg KA, Carl CS, Jeppesen JF, Wojtaszewski JFP, et al. Exercise increases circulating GDF15 in humans. Mol Metab 2018;9:187–91. https://doi.org/10.1016/j.molmet.2017.12.016.
- [51] Macia L, Tsai VW-W, Nguyen AD, Johnen H, Kuffner T, Shi Y-C, et al. Macrophage inhibitory cytokine 1 (MIC-1/GDF15) decreases food intake, body weight and improves glucose tolerance in mice on normal & obesogenic diets. PLoS ONE 2012; 7:e34868. https://doi.org/10.1371/journal.pone.0034868.